

Level-crossing statistics of a passive scalar dispersed in a neutral boundary layer

*Original*

Level-crossing statistics of a passive scalar dispersed in a neutral boundary layer / Bertagni, Matteo B.; Marro, Massimo; Salizzoni, Pietro; Camporeale, CARLO VINCENZO. - In: ATMOSPHERIC ENVIRONMENT. - ISSN 1352-2310. - 230:(2020). [10.1016/j.atmosenv.2020.117518]

*Availability:*

This version is available at: 11583/2813672 since: 2020-04-20T10:11:06Z

*Publisher:*

Elsevier

*Published*

DOI:10.1016/j.atmosenv.2020.117518

*Terms of use:*

This article is made available under terms and conditions as specified in the corresponding bibliographic description in the repository

*Publisher copyright*

(Article begins on next page)

# Level-crossing statistics of a passive scalar dispersed in a neutral boundary layer

Matteo B. Bertagni<sup>a</sup>, Massimo Marro<sup>b</sup>, Pietro Salizzoni<sup>b</sup>, Carlo Camporeale<sup>a</sup>

<sup>a</sup>*Department of Land, Infrastructure and Environmental Engineering, Politecnico di Torino, Corso Duca degli Abruzzi 24, 10124, Torino, Italy*

<sup>b</sup>*Laboratoire de Mécanique des Fluides et d'Acoustique, University of Lyon, CNRS UMR 5509 Ecole Centrale de Lyon, INSA Lyon, Université Claude Bernard, 36, avenue Guy de Collongue, 69134 Ecully, France*

---

## Abstract

The concentration of a passive scalar dispersed in a turbulent flow exhibits a complex stochastic dynamics. In this paper, we present a minimalist stochastic model that resembles the concentration statistics of a passive scalar emitted from a localized source in a neutral boundary layer. The model provides closed forms for the crossing rates and times – the mean frequency of exceeding a certain concentration level and the mean time above it–. Three concentration statistics are needed as model inputs: the mean, the standard deviation, and the integral scale. By giving analytical relationships also for these statistics, we provide a completely closed methodology that may serve as a rapid and practical tool to estimate the dynamics of a pollutant dispersed in the atmosphere. Results are validated against wind-tunnel measurements.

*Keywords:* Crossing rates, Crossing Times, Gamma distribution, Analytical relationships, Turbulent dispersion

---

## 1. Introduction

Turbulent flows are responsible for the chaotic mixing of many “substances” of natural and anthropic origins. Pollutants, heat, air moisture and combustible chemicals are just some examples. In many cases, the substance does not affect the fluid flow, so that it may be referred to as a *passive scalar*. On the opposite, the fluid flow causes the passive scalar to exhibit a complex turbulent dynamics (Fig. 1), whose many physical and statistical aspects

8 still need to be unveiled. For the wide-ranging implications of scalar turbu-  
 9 lence, many reviews have been dedicated to the subject in the last years, see  
 10 [1, 2, 3, 4, 5] and references therein.

11 In the atmospherical sciences, the crucial features of scalar turbulence re-  
 12 gard the statistics of pollutant and odour concentrations due to both natural  
 13 and anthropogenic releases. The knowledge of these statistics is necessary,  
 14 for instance, to determine the risk for human health generated by a toxic  
 15 substance [6, 7, 8] or the level of annoyance induced by a nuisance odor  
 16 [9, 10, 11].

17 Regarding the one-point statistics of the passive scalar concentration  
 18  $C[\mathbf{x}, t]$ , several analytical models for the probability density function (PDF)  
 19 have been tested in the last decades against laboratory and field data [e.g.,  
 20 12, 13, 14]. The conclusion on which distribution better fits the data usually  
 21 depends on the experimental setup. Yet, recent results [e.g 15, 16, 17, 18]  
 22 have been converging on the choice of the Gamma distribution as the best  
 23 fit for the PDF of a passive scalar concentration released from a point source  
 24 in a neutral boundary layer

$$p_{\Gamma} = \frac{\lambda^{\lambda} C^{\lambda-1}}{\Gamma[\lambda] \mu^{\lambda}} e^{-\lambda C/\mu}, \quad (1)$$

25 where  $\lambda = \mu^2/\sigma^2$ ,  $\mu$  is the mean value,  $\sigma^2$  the variance, and  $\Gamma[\cdot]$  is the Gamma  
 26 special function [19]. Furthermore, the Gamma distribution has also been  
 27 observed to well fit the one-point PDF of concentration in confined turbulence  
 28 [20, 21]. For practical goals, the Gamma distribution is an encouraging result  
 29 as by just defining the first two statistical moments of  $C$ , all the one-point  
 30 statistics can be defined in an analytical and expeditious way.

31 Nonetheless, the knowledge of the PDF does not provide any information  
 32 on the temporal dynamics of the concentration, which is fundamental for  
 33 several purposes. For example, the exposure times are necessary to spec-  
 34 ify the risk for human health related to an airborne toxic substance –toxic  
 35 load=concentration×exposure time– [e.g. 7, 8]. Additionally, the annoyance  
 36 induced by nuisance odours, which are nowadays classified as atmospheric  
 37 pollutants by several jurisdictions [22], is controlled by the frequency of oc-  
 38 currence of whiffs. In fact, the human nose becomes insensitive to smells to  
 39 which is continuously subjected, so that low concentration smells at irreg-  
 40 ular intervals of time are actually more disturbing than a constant higher-  
 41 concentration smell [23].

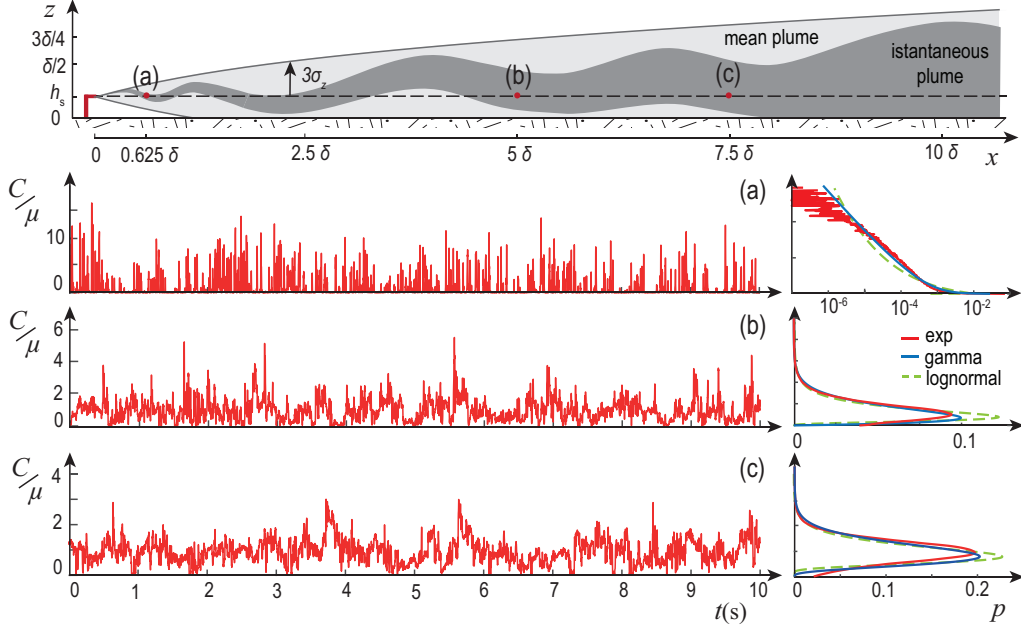


Figure 1: Sketch of the emission conditions and examples of experimental concentration time-series with their PDFs. The experimental PDFs are in solid red lines. The Gamma and Lognormal distributions are in solid-blue and dashed-green lines, respectively.  $t(s)$  is time in seconds. Notice that only the first 10 seconds of the 15 minutes concentration series are shown (Elevated Source with 6 mm diameter from Bertagni et al. [18]).  $\delta$  and  $h_s$  are the boundary-layer and source heights, respectively).

The first attempt to address the temporal statistics of a passive scalar involved a fluctuating plume model calibrated with experiments [24]. Successively, some studies [25, 26] tried to use Rice's theory [27] to relate the upcrossing rates to the joint PDF of the concentration and its time derivative. However, this latter PDF is generally unknown, making Rice's theory difficult to apply. A notable exception was provided by Yee [28], who derived closed relationships for the upcrossing rates (and times) by using Rice's theory under the assumption of a Lognormal PDF for the in-plume concentration fluctuations (see Appendix A for further details). Yet, the Gamma distribution (1) is usually a better model than the Lognormal, as shown in Fig. 1 and also pointed out in previous publications [e.g. 16, 29].

More recently, the research has focused on numerical stochastic models [30, 31, 32, 33], which nicely reproduce the concentration time-series, but offer no analytical solution for the level-crossing statistics. In general, these

stochastic models require a PDF and a time-scale to be set. These quantities are usually evaluated from experiments, empirical relations or Lagrangian micro-mixing models [33].

In this Paper, we provide a simple stochastic model for the concentration dynamics in which the steady-state PDF is the Gamma distribution (1) and the crossing rates and times, i.e., the mean frequency of exceeding a certain concentration level and the mean time above it, are given in closed form. Three one-point statistics need to be set in the model: the mean  $\mu$ , the standard deviation  $\sigma$ , and the temporal integral-scale  $\tau$ . The latter is defined as the integral of the autocorrelation function of  $C$ , and can be interpreted as the temporal memory of the one-point concentration dynamics [34]. First, we use wind-tunnel data [16, 18] to evaluate the triad  $(\mu, \sigma, \tau)$  and to verify the analytical relationship for the crossing rates and times (see the Appendix B for a brief description of the experimental setup). Second, we evaluate the triad  $(\mu, \sigma, \tau)$  through analytical relationships, among which the one for the Eulerian time-scale  $\tau$  is a novelty. In this way, we provide a fully closed model for the evaluation of the recurrence statistics of a passive scalar dispersed in a turbulent flow.

## 2. The Stochastic Model

According to a well-established theoretical framework [35], the turbulent dispersion of a fluctuating plume is phenomenologically driven by two main physical processes: the transport by turbulent eddies of the plume centroid, or centre of mass, and the relative dispersion around it. The former process, also referred to as *meandering*, is fundamental in the proximity of the source, where the plume has a small size and is transported as a whole by turbulent eddies. The resulting one-point concentration time-series (Fig. 1a) exhibits a very intermittent signal with random shots induced by the passage of the turbulent eddies transporting the passive scalar. Very far from the source, the plume has spread enough to englobe these eddies, so that the intermittent action of the meandering process becomes negligible with respect to the homogenization induced by the *relative dispersion* (Fig. 1c). In between the near and the far field, the intermediate plume size causes both processes –meandering and relative dispersion– to be essential in the concentration dynamics (see Fig. 1b, where the low-intensity shots induced by the meandering are still recognizable).

91 From these considerations, we define a stochastic model for the concen-  
 92 tration dynamics that takes into account the two physical processes and  
 93 guarantees the Gamma distribution (1) as the steady-state PDF. This is the  
 94 Compound Poisson Process (CPP) with linear losses

$$dC = -\frac{C}{\tau}dt + d\zeta, \quad (2)$$

95 where  $t$  is time and  $\tau$  is the integral time-scale. The stochastic term  $d\zeta$  is  
 96 a white shot noise [e.g. 34] that represents the sequence of pulses at ran-  
 97 dom times induced by the turbulent eddies (meandering). The shot intensity  
 98 and the time interval between subsequent shots are extracted from space-  
 99 dependent exponential PDFs with mean values  $\sigma^2/\mu$  and  $\tau\sigma^2/\mu^2$ , respec-  
 100 tively [e.g. 36]. The deterministic part of (2) recalls the relative-dispersion,  
 101 or micro-mixing, models [e.g. 37, 38]), but without the relaxation of the  
 102 concentration towards a mean value.

103 A crucial advantage of the CPP is analytical tractability. In particular,  
 104 the upcrossing time  $T_\phi^+$ , which is the average time  $C$  stays above a certain  
 105 threshold level  $\phi$ , is known in closed form

$$T_\phi^+ = \tau e^{\phi\lambda/\mu} E[1 - \lambda, \lambda\phi/\mu], \quad (3)$$

106 where  $E[n, m] = \int_1^\infty \exp[-ms]/s^n ds$  is the exponential integral function [19].  
 107 The upcrossing rate  $N_\phi^+$ , which is the mean frequency of upcrossing the  
 108 threshold level  $\phi$ , can be readily obtained as

$$N_\phi^+ = \frac{P_\phi^+}{T_\phi^+} = \frac{(\lambda\phi/\mu)^\lambda \exp[-\lambda\phi/\mu]}{\tau \Gamma[\lambda]}, \quad (4)$$

109 where  $P_\phi^+$  is the probability of  $C > \phi$ , known from eq. (1). Equivalently,  
 110 one could address the downcrossing rate  $N_\phi^-$  and time  $T_\phi^-$ , which are the  
 111 mean frequency of downcrossing the level  $\phi$  and the average time below it.  
 112 In particular,  $N_\phi^+ = N_\phi^-$ , and thus  $T_\phi^- = T_\phi^+ P_\phi^-/P_\phi^+$ , where  $P_\phi^- = 1 - P_\phi^+$  is the  
 113 probability of  $C < \phi$ . However, for the more important practical purposes, we  
 114 herein focus the analysis on the upcrossing statistics (in the paper we often  
 115 use the term *crossing* in place of *upcrossing*).

116 Equations (3) and (4) provide an easy and ready-to-use tool to evaluate  
 117 the upcrossing times and rates in every spatial point of interest starting from  
 118 the triad  $(\mu, \sigma, \tau)$ .

### 119 3. Analytical closures

120 To provide a closed-methodology to evaluate the crossing times (3) and  
 121 rates (4), we here give the analytical relationships for the triad  $(\mu, \sigma, \tau)$ .

122 *The mean  $\mu$ .* For a passive scalar released from a point source at  $(x, y, z) =$   
 123  $(0, 0, h_s)$ , the mean field  $\mu$  is well reproduced by the classical Gaussian model

$$\mu = c \exp \left[ -\frac{y^2}{2\sigma_y^2} \right] \left( \exp \left[ -\frac{(z - h_s)^2}{2\sigma_z^2} \right] + \exp \left[ -\frac{(z + h_s)^2}{2\sigma_z^2} \right] \right), \quad (5)$$

where  $c = \dot{M} / (2\pi\sigma_y\sigma_z U_s)$ ,  $U_s$  is the mean velocity at the source height, and  $\dot{M}$  is the passive scalar mass flux emitted at the source. The presence of the lower boundary has been included in (5) through a mirror imaginary source at  $z = -h_s$  [e.g. 39].  $\sigma_y$  and  $\sigma_z$  define the transversal and vertical mean plume spread, which, in the absence of experimental measurements, can be defined through the standard Taylor's approach [40]

$$\sigma_y^2 = \frac{d_s^2}{6} + 2\sigma_v^2 T_{L,v} \left[ t_f - T_{L,v} \left( 1 - \exp \left[ -\frac{t_f}{T_{L,v}} \right] \right) \right], \quad (6)$$

$$\sigma_z^2 = \frac{d_s^2}{6} + 2\sigma_w^2 T_{L,w} \left[ t_f - T_{L,w} \left( 1 - \exp \left[ -\frac{t_f}{T_{L,w}} \right] \right) \right], \quad (7)$$

124 where  $\sigma_v^2$  and  $\sigma_w^2$  are the variances of the transverse and vertical velocities,  
 125 respectively,  $d_s$  is the source diameter,  $t_f = x/U_s$  is the flight time,  $T_{L,v} =$   
 126  $2\sigma_v^2/(\varepsilon C_0)$  and  $T_{L,w} = 2\sigma_w^2/(\varepsilon C_0)$  are the Lagrangian transverse and vertical  
 127 time scales, being  $\varepsilon$  the turbulent kinetic energy dissipation rate and  $C_0 = 4.5$   
 128 the Kolmogorov constant [41, 16].

129 In Fig. 2, a graphical comparison between experimental and theoretical  
 130 results for  $\mu$  is reported (red lines and symbols).

131 *The variance  $\sigma^2$ .* In a recent article [18], we have obtained an analytical  
 132 solution for  $\sigma^2$  from the transport equation of the PDF  $p$  of the passive-  
 133 scalar concentration

$$U_s \partial_x p = (K_y \partial_y^2 + K_z \partial_z^2) p + \tau_m^{-1} \partial_\psi [p(\psi - \mu)], \quad (8)$$

134 where  $K_y = d\sigma_y^2/2dt$  and  $K_z = d\sigma_z^2/2dt$  are the transversal and vertical tur-  
 135 bulent diffusivities, respectively, and  $\tau_m$  is the mixing time-scale.  $\psi$  is the  
 136 sample space variable of the concentration, i.e., the collection of all possible

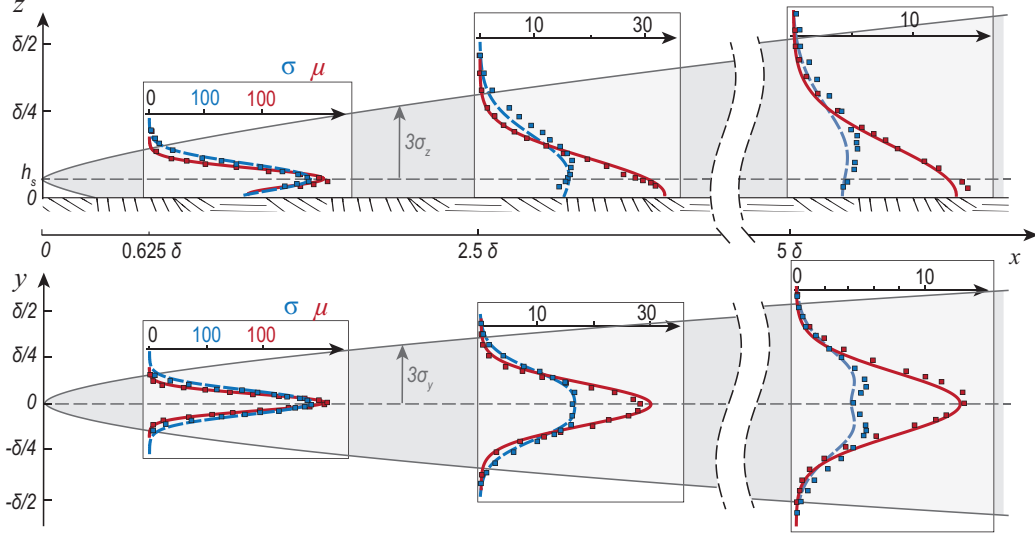


Figure 2: Vertical and transverse profiles of the mean  $\mu$  (red) and the standard deviation  $\sigma$  (blue) of the concentration. Solid-red lines come from equation (5) for  $\mu$ . Dashed-blue lines come from equation (9) for  $\sigma$ . Symbols correspond to experimental data LLS3 [16]. Concentration is here scaled with  $\dot{M}U_s^{-1}\delta^{-2}$ , being  $\dot{M}$  the mass flux emitted at the source.

137 outcomes of  $C$ . In eq. (8), the turbulent fluxes have been closed through a  
 138 classical gradient-diffusion model, and the effect of molecular diffusion in the  
 139 passive scalar mixing has been included through an Interaction by Exchange  
 140 with the Mean (IEM) model [e.g. 42]. By solving the transport equation of  
 141 the the statistical moments of concentration, derived from eq. (8), Bertagni  
 142 et al. [18] obtained

$$\sigma^2 = \frac{2c^2x^2}{\tau_m U_s} \int_{\xi}^x \left( \frac{\exp \left[ -2 \frac{(x-x_0)}{\tau_m U_s} - \frac{x}{(2x-x_0)} \left( \frac{y^2}{\sigma_y^2} + \frac{(z-h_s)^2}{\sigma_z^2} \right) \right]}{x_0(2x-x_0)} + r_{\sigma} \right) dx_0 - \mu^2, \quad (9)$$

143 where  $\xi$  is the source parameter, and  $r_{\sigma}$  is the reflection term

$$r_{\sigma} = \frac{\exp \left[ -2 \frac{(x-x_0)}{U_s \tau_m} - \frac{x}{2x-x_0} \left( \frac{y^2}{\sigma_y^2} + \frac{(z+h_s)^2}{\sigma_z^2} \right) \right]}{x_0(2x-x_0)} \left( 1 + 2 \exp \left[ \frac{2h_s x (h_s x_0 + x_0 z - h_s x)}{x_0(2x-x_0)\sigma_z^2} \right] \right). \quad (10)$$

144 We invite the reader to refer to the original publication for further details  
 145 on the derivation of (9). From dimensional analysis and best fitting with  
 146 experiments, we found  $\xi = \delta (d_s/h_s)^{10}$  for the source parameter [18]. Regard-



147 ing the mixing time-scale  $\tau_m$ , the IEM model is known to introduce spurious  
 148 fluxes that alter the concentration statistics [e.g. 37, 43]. Yet, Bertagni et al.  
 149 [18] have shown that this issue can be avoided for the present model of  $\sigma^2$   
 150 by considering two formulations for the mixing time-scale. In the near field,  
 151 where meandering enhances concentration fluctuations ( $\sigma/\mu > 1$ ), the mix-  
 152 ing time-scale may be considered constant and proportional to the turbulent  
 153 time-scale, i.e.,  $\tau_m \propto k/\varepsilon$ , where  $k$  is the turbulent kinetic energy and  $\varepsilon$  its  
 154 rate of dissipation. Instead, a more complicated model for  $\tau_m$ , which ac-  
 155 counts for its spatial dependence, is needed in the far field, where relative  
 156 dispersion dampens the passive scalar fluctuations ( $\sigma/\mu < 1$ ). Eventually, the  
 157 mixing time-scale is here evaluated as

$$\tau_m = \begin{cases} \alpha_1 k/\varepsilon, & \text{for } \sigma/\mu > 1, \\ \alpha_2 \sigma_r/\sigma_{ur}, & \text{for } \sigma/\mu < 1, \end{cases} \quad (11)$$

where the constants  $\alpha_1 = 0.44$  and  $\alpha_2 = 0.65$  have been obtained by a fit-  
 ting with the wind-tunnel experiments,  $\sigma_r$  is an isotropic length scale of the  
 plume spread, and  $\sigma_{ur}$  is the r.m.s. of the relative velocity fluctuations (the  
 difference between the turbulent velocity and the instantaneous velocity of the  
 plume centre of mass). The formulation for  $\sigma/\mu < 1$  in (11) originally  
 comes from the work by Cassiani et al. [38] and has been later used also in  
 numerical simulations of dispersing plumes [e.g. 44]. The quantities involved  
 in (11) are modelled as

$$\sigma_{ur}^2 = \sigma_u^2 (\sigma_r/L_E)^{2/3}, \quad (12)$$

$$\sigma_r^2 = \frac{C_r \varepsilon (t_0 + t_f)^3}{1 + (C_r \varepsilon (t_0 + t_f)^3 - d_s^2)/(d_s^2 + 2\sigma_u T_L t_f)}, \quad (13)$$

158 where  $L_E = (3\sigma_u/2)^{3/2} \varepsilon$  is the Eulerian integral length-scale,  $t_0 = (d_s^2/C_r \varepsilon)^{1/3}$   
 159 is the inertial formulation for a dispersion from a finite source size [45],  $C_r =$   
 160 0.3 is the Richardson constant [44], and  $\sigma_u^2$  is calculated, because of the  
 161 inhomogeneity of the turbulent field, as the average of the variances of the  
 162 three velocity components. Notice that when the plume size reaches the  
 163 Eulerian integral length-scale, i.e.,  $\sigma_r = L_E$ , meandering becomes negligible  
 164 with respect to relative dispersion in the plume spread, so that  $\sigma_{ur} = \sigma_u$ .

165 In Fig. 2, a graphical comparison between experimental and theoretical  
 166 results for  $\sigma$  is reported (blue lines and symbols).

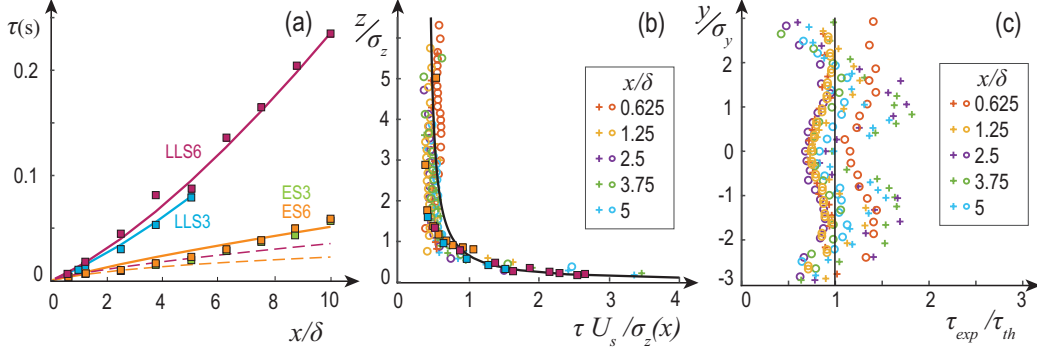


Figure 3: Integral time-scale  $\tau$ . The solid lines come from eq. (14) and the symbols from several setups of the wind-tunnel experiments [16, 18]. (a) Integral time-scale  $\tau$  on the plume axis ( $y=0$ ,  $z=h_s$ ) at increasing distances from the source. The dashed lines show  $\tau$  from eq. (14) without the effect of the ground reflection ( $r_\tau = 0$ ). (b) Vertical profiles at several distances from the source of the scaled integral scale  $\tau$  ( $y=0$ ). The solid lines highlight the autosimilar trend  $\alpha_3(1 + r_\tau)$ . Circles and crosses are from the ES6 and LLS3 cases by Nironi et al. [16], respectively. Filled squares are the experimental  $\tau$  at the source height. (c) Transversal profiles at the source height ( $z=h_s$ ) of the ratio between experimental and theoretical  $\tau$ .

167 *The integral time-scale  $\tau$ .* The third parameter, i.e., the integral of the auto-  
 168 correlation function of  $C$ , can be interpreted as the temporal memory of the  
 169 one-point concentration dynamics [34]. This Eulerian time-scale is usually  
 170 defined through an empirical relationship that links it to the plume size and  
 171 the mean velocity  $U$  [e.g. 46, 33, 47]. Indeed, the temporal correlation of  
 172 the concentration series is crucially related to the plume spread. Near the  
 173 source, in the meandering-dominated regime, the concentration signal is very  
 174 low correlated (Fig. 1a). Further from the source, as the plume spreads and  
 175 englobes the turbulent eddies, the one-point concentration signal increases  
 176 its temporal correlation (Fig. 1b-c) [47]. This increasing trend of the tem-  
 177 poral correlation with the distance from the source is also evident from the  
 178 experiments (see symbols in Fig. 3a).

179 Here, we provide a novel model for  $\tau$  that accounts for the presence of the  
 180 lower boundary and the consequent vertical anisotropy of the turbulent field.  
 181 For this reason, we adopt the vertical plume spread  $\sigma_z$  as the spatial scale  
 182 of reference. Accordingly, the normalized integral scale  $\tau U_s / \sigma_z$  is reported  
 183 for several vertical profiles and the two experimental setups in Fig. 3b. The  
 184 results show a self-similar behavior, which highlights the effect of the lower

185 boundary and the consequent anisotropy of the turbulent field. Notice that,  
 186 because of the  $x$ -dependence of  $\sigma_z$ , the same  $z$  value corresponds to different  
 187 positions in the axis  $z/\sigma_z$  when several  $x$ -profiles are reported (the filled  
 188 squares in Fig. 3b are the integral scales at the source height  $h_s$ ). Eventually,  
 189 from Fig. 3b, we obtain to the following relationship for  $\tau$

$$\tau = \alpha_3 \frac{\sigma_z}{U_s} (1 + r_\tau), \quad (14)$$

190 where  $\alpha_3 = 0.4$ , and the term  $r_\tau = (\sigma_z/z)$  stands for the reflection induced  
 191 by the lower boundary, which smooths the concentration fluctuations thus  
 192 increasing the temporal correlation of the concentration signal. Neglecting  
 193 the lower boundary ( $r_\tau = 0$ ) causes an high underestimation of the integral  
 194 scale  $\tau$ . This is evident in Fig. 3a, where  $\tau$  at the source height  $h_s$  is reported  
 195 for several experimental setups (solid lines for  $r_\tau = (\sigma_z/z)$  and dashed lines  
 196 for  $r_\tau = 0$ ). For completeness, we also report the transversal dependency of  
 197  $\tau$  in Fig. 3c. Most of the experimental data in the scaled coordinates are  
 198 sparse around 1. Thus, for simplicity, the  $y$ -dependence of  $\tau$  is neglected.

#### 199 4. Model application

200 The Compound Poisson Process (2) provides the analytical relationships (3)  
 201 and (4) to evaluate the upcrossing times and rates. We compare the valid-  
 202 ity of these relationships (lines) with wind-tunnel data (symbols) in Fig. 4  
 203 and 5 (see the Appendix B for a brief description of the experimental setup  
 204 and dataset). The only input required is the triad  $(\mu, \sigma, \tau)$ , which we de-  
 205 fine through two strategies: i) the experimental values (solid blue lines), ii)  
 206 the analytical closures (5)-(9)-(14) (black-dotted lines). The first strategy  
 207 highlights the validity of the CPP model in reproducing the level-crossing  
 208 statistics. The second strategy shows the efficiency of a completely analyt-  
 209 ical approach. We may notice that, as the closed relationships (5)-(9)-(14)  
 210 provide good estimates for the triad (see also Fig. 2 and 3), the dotted-black  
 211 and solid-blue lines are very much alike.

212 Overall, the crossing times monotonically decrease with the concentration  
 213 level. Instead, the crossing rates exhibit a maximum close to the mean con-  
 214 centration value, as around it the concentration signal normally evolves. The  
 215 agreement between model and experiment is good throughout the domain of  
 216 plume dispersion for both the Elevated Source (ES) and the Low Level Source

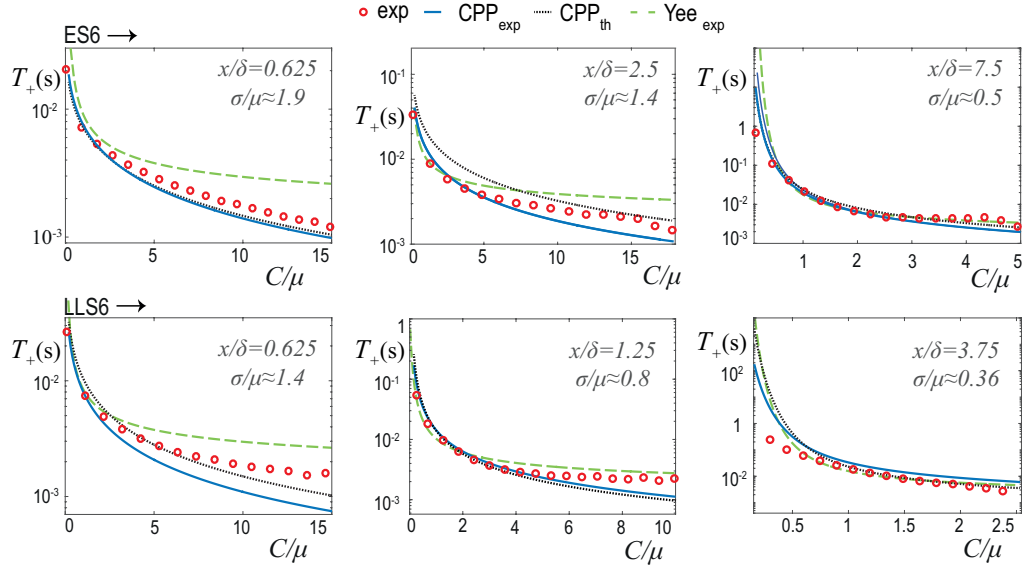


Figure 4: Comparison of experimental (symbols) and theoretical (lines) upcrossing times  $T^+$  on the plume axis for two source configurations. The blue-solid lines ( $\text{CPP}_{\text{exp}}$ ) come from eq. (3) with the experimental values for the triad  $(\mu, \sigma, \tau)$ . The dotted-black lines ( $\text{CPP}_{\text{th}}$ ) come from eq. (3) with the values for the triad  $(\mu, \sigma, \tau)$  obtained from the theoretical eqs. (5)-(9)-(14). The dashed-green lines come from the model by Yee [28] (Appendix A) with experimental values for the triad.

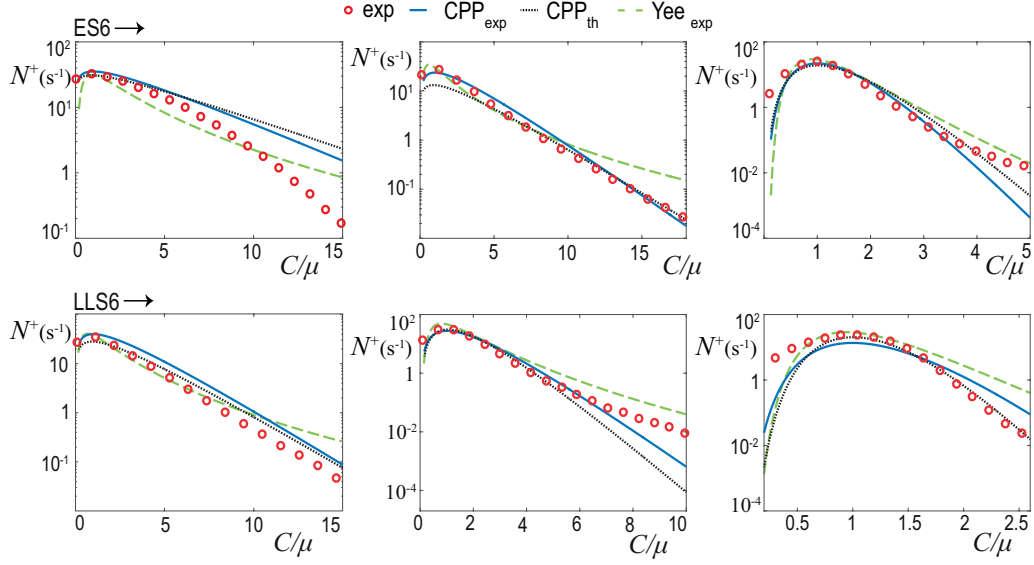


Figure 5: Comparison of experimental (symbols) and theoretical (lines) upcrossing rates  $N^+$  for the same points of Fig. 4. The blue-solid lines ( $\text{CPP}_{\text{exp}}$ ) come from eq. (4) with the experimental values for the triad  $(\mu, \sigma, \tau)$ . The dotted-black lines ( $\text{CPP}_{\text{th}}$ ) come from eq. (4) with the values for the triad  $(\mu, \sigma, \tau)$  obtained from the theoretical eqs. (5)-(9)-(14). The dashed-green lines come from the model by Yee [28] (Appendix A) with experimental values for the triad.

(LLS), with numbering referring to the source diameter in mm. Some deviations in the comparison are visible for the peak concentration values in the close field ( $\sigma/\mu \gg 1$ ). Nonetheless, the results are encouraging considering the simplicity of the stochastic model adopted and the approximations made to obtain the analytical relationships (5)-(9)-(14).

Additionally, we have included the results obtained through the model by Yee [28] (dashed-green lines). He achieved analytical relationships for the crossing times and rates by using Rice's theory under the assumption of a Lognormal distribution for the concentration. Also Yee's model needs three concentration statistics as input: the mean  $\mu$ , the variance  $\sigma^2$ , and a time-scale  $t_T$  (see Appendix A). We have used the experimental values for this triad, so that the dashed-green lines ( $Yee_{\text{exp}}$ ) should be compared to the solid-blue lines ( $CPP_{\text{exp}}$ ). Although both models show some inaccuracy, the CPP seems to yield better trends for the crossing rates and times. This is probably due to the better performance of the Gamma distribution with respect to the Lognormal one (see the panels in Fig. 1).

We wish to further add a comment about the role of intermittency. Near the source, the concentration signals show periods of zero concentration caused by the meandering motion of the plume. From a rigorous mathematical point of view, the PDF of the intermittent concentration signal should be composed by a proper model (e.g., the Gamma  $p_r$ ) for the distribution of the in-plume concentration fluctuations ( $C > 0$ ) and an atom of probability in  $C = 0$ , i.e.,  $p = \Upsilon p_r + (1 - \Upsilon)\delta[C]$ , where  $\Upsilon = P_0^+$  is the intermittency factor and  $\delta[\cdot]$  is the Dirac's delta. However, several reasons induced us to not formally include intermittency in our model: i) for the practical purposes of evaluating the probability of peak events and their average duration, it is indifferent if the probability of low values of concentration lies exactly in  $C = 0$  or in a positive small interval of 0 (notice that  $p_r \rightarrow \infty$  for  $C \rightarrow 0$ ); ii) as  $\Upsilon$  depends on the small-scale structures of turbulence [e.g. 48], its evaluation in laboratory and field experiments is strongly arbitrary (normally is defined as  $\Upsilon = P_\epsilon^+$ , where  $\epsilon$  is an arbitrarily small value [16]) and, to the authors' knowledge, no reliable theoretical models are currently available; iii) we repeated the analysis including the experimental intermittency factor (with  $\epsilon = \mu/100$ ) and the so-obtained level-crossing statistics were within a relative difference of at maximum 30% (indeed the order of  $1 - \Upsilon$ ). For these reasons and in favor of simplicity, we did not explicitly include intermittency in our mathematical formulation. However, we point out that we used our experimental results for the intermittency factor (with  $\epsilon = \mu/100$ )

in the analytical relationships by Yee. This was necessary, especially in the meandering regime (first columns of panels in Figures 4 and 5), because of an intrinsic limit of the the Lognormal distribution, which tends to 0 for  $C \rightarrow 0$  and partially loses the information about the probability of low values of concentration.

## 5. Conclusions

In this paper, the Compound Poisson Process (2) is used to obtain analytical level-crossing statistics for a passive scalar released from a point source in a neutral boundary-layer. Indeed, the minimalist model (2) provides the Gamma distribution (1) as the steady-state PDF and the analytical relationship (3) and (4) for the average crossing times  $T_\phi^+$  and rates  $N_\phi^+$ . The validity of these results is verified by comparison with wind-tunnel data in Figs. 4 and 5.

Additionally, we have provided analytical relationships for the three input parameters of the model: the mean  $\mu$ , which is well resembled by the classical Gaussian model of plume dispersion (5); the variance  $\sigma^2$ , determined through the relationship (9) by Bertagni et al. [18]; and the integral scale  $\tau$ , for which we propose the novel model (14). Clearly, more complicated numerical approaches (e.g. Reynolds-averaged Navier-Stokes equations) could be adopted to define the concentration statistics  $\mu$  and  $\sigma$  to be used within the model for  $T_\phi^+$  and  $N_\phi^+$ . Yet, we wished to propose a closed-methodology to obtain the level-crossing statistics for the passive scalar dynamics by just knowing the emission condition at the source and the velocity field.

The methodology here presented may serve as a rapid and practical tool to estimate the dynamics of a substance dispersed in the atmosphere. A possible application could be the extension of analytical operational models (e.g., AERMOD or ADMS [49, 50]), which are currently used for the assessment of chronic risks associated to the mean (time-averaged over an hourly interval) concentration of exposure. Starting from the closed solutions for the level-crossing statistics here proposed, the skills of these operational models could be extended to the estimate of accidental risks, which are intimately linked with the probability of exceeding a certain concentration threshold. Furthermore, the present methodology could also benefit to the assessment of nuisance odour dispersion, whose measurement in the field remains nowadays a complicated task [e.g. 9].

290 Future research should possibly expand the present analysis of average  
 291 level-crossing statistics to their probability distribution functions. Field mea-  
 292 surements [51] suggested that a Lognormal distribution could be suitable for  
 293 the purpose, but this would require an additional theoretical definition for  
 294 the variance of level-crossing statistics. The same field-measurements also in-  
 295 dicated that, when level-crossing statistics are considered, stable boundary-  
 296 layers resemble neutral boundary-layers at further distance from the source.  
 297 Yet, extensions of the present theory to non-neutral boundary-layers and dif-  
 298 ferent emission conditions (e.g., line or distributed sources) remain an open  
 299 challenge.

### 300 Appendix A. Resume of Yee's (2000) model

301 We here give the analytical results obtained by Yee [28] and used within  
 302 this paper for a comparison with our model. We invite the reader to refer to  
 303 the original publication for further details. Yee used Rice's theory [27] under  
 304 the assumption of a Lognormal distribution for the in-plume concentration  
 305 ( $C > 0$ )

$$p_{\log} = \frac{1}{C \sqrt{2\pi \log[\beta]}} \exp \left[ -\frac{(\log[C] - \log[\mu/\sqrt{\beta}])^2}{2 \log[\beta]} \right], \quad (\text{A.1})$$

where  $\beta = 1 + \sigma^2/\mu^2$ . Starting from this assumption, Yee obtained a closed form for the joint PDF of the concentration  $C$  and its time derivative  $dC/dt$ , which is required by Rice's theory. Eventually, Yee provided the following analytical expressions for the crossing rates and times

$$N_{\phi}^{+} = \frac{\sigma}{2\pi \mu t_T} \frac{\exp \left[ -\log^2 \left[ \sqrt{\beta} \phi / \mu \right] / (2 \log[\beta]) \right]}{\sqrt{\beta \log[\beta]}}, \quad (\text{A.2})$$

$$T_{\phi}^{+} = P_{\phi}^{+} / N_{\phi}^{+}, \quad (\text{A.3})$$

where  $P_{\phi}^{+}$  is the probability of  $C > \phi$ , defined from eq. (A.1). The time scale  $t_T$ , to which Yee referred to as Taylor micro-time scale, is defined as

$$t_T = \frac{\sigma}{\sigma_{C'}}, \quad (\text{A.4})$$

306 where  $\sigma_{C'}$  is the r.m.s. of the concentration time derivative  $dC/dt$ , which  
 307 requires experimental or field measurements. We stress out that these math-  
 308 ematical results were originally derived just for in-plume concentration fluc-  
 309 tuations ( $C > 0$ ). However, they can be extended to an intermittent con-  
 310 centration signal ( $C \geq 0$ ) by considering the in-plume, instead of the total,



mean and variance, and the intermittency factor (as Yee suggested in the conclusion of his paper). Accordingly, we have included the experimental results for the intermittency in the evaluation of the level-crossing statistics in the meandering regime (first columns of panels in Figures 4 and 5).

## Appendix B. Brief Description Of The Experimental Setup

The experimental data used within this paper were collected and analyzed in Nironi et al. [16] and Bertagni et al. [18]. The experiments were run in the atmospheric wind tunnel of the Laboratoire de Mécanique des Fluides et d’Acoustique at the Ecole Centrale de Lyon, in France. This is a recirculating wind tunnel 14 m long, 2.5 m high, and 3.7 m wide, in which a neutrally-stratified boundary layer of height  $\delta=0.8$  m and free-stream velocity  $U_\infty=5$  m s<sup>-1</sup> was generated. Ethane ( $C_2H_6$ ) was used as a tracer in the experiments, since it has a density similar to air, and was continuously discharged from a source of varying diameter and elevation. As in Nironi et al. [16], Bertagni et al. [18], the following notation is used for the source configuration: Elevated Source (ES3 and ES6,  $h_s=152$  mm), Lower Level Source (LLS3,  $h_s=48$  mm, LLS6,  $h_s=40$  mm). The numbers in the acronyms stay for the diameter in mm. We stress out that the concentration time-series used to obtain Fig. 4 and 5 were measured on the plume axis for 15 minutes with a sampling frequency of 1000 Hz, to assure statistical convergence to the crossing times. Instead the time-series by Nironi et al. [16] are 5 minutes long. The full experimental dataset is available at <http://air.ec-lyon.fr/>.

## References

- [1] B. Shraiman, E. Siggia, Scalar turbulence, *Nature* 405 (2000) 639.
- [2] Z. Warhaft, Passive scalars in turbulent flows, *Ann. Rev. Fluid Mech.* 32 (2000) 203–240.
- [3] P. E. Dimotakis, Turbulent mixing, *Annu. Rev. Fluid Mech.* 37 (2005) 329–356.
- [4] K. R. Sreenivasan, Turbulent mixing: A perspective, *Proc. Nat. Acad. Science* (2018) 201800463.
- [5] E. Villiermaux, Mixing Versus Stirring, *Ann. Rev. Fluid Mech.* 51 (2019) 245–273.

- 343 [6] M. Kampa, E. Castanas, Human health effects of air pollution, *Environ.*  
344 *Pollut.* 151 (2008) 362–367.
- 345 [7] D. R. Sommerville, K. H. Park, M. O. Kierzewski, M. D. Dunkel, M. I.  
346 Hutton, N. A. Pinto, Toxic load modeling, *Inhalation Toxicology* (2006)  
347 137–158.
- 348 [8] A. Gunatilaka, A. Skvortsov, R. Gailis, A review of toxicity models for  
349 realistic atmospheric applications, *Atmospheric environment* 84 (2014)  
350 230–243.
- 351 [9] L. Capelli, S. Sironi, R. Del Rosso, J.-M. Guillot, Measuring odours in  
352 the environment vs. dispersion modelling: A review, *Atmos. Environ.*  
353 79 (2013) 731–743.
- 354 [10] D. Oetl, E. Ferrero, A simple model to assess odour hours for regulatory  
355 purposes, *Atmos. Environ.* 155 (2017) 162–173.
- 356 [11] M. Ravina, D. Panepinto, J. M. Estrada, L. De Giorgio, P. Salizzoni,  
357 M. Zanetti, L. Meucci, Integrated model for estimating odor emissions  
358 from civil wastewater treatment plants, *Environ. Sci. Pollut. R.* (2019)  
359 1–16.
- 360 [12] B. Sawford, Conditional concentration statistics for surface plumes in  
361 the atmospheric boundary layer, *Boundary-Layer Meteorol.* 38 (1987)  
362 209–223.
- 363 [13] E. Yee, D. Wilson, B. Zelt, Probability distributions of concentration  
364 fluctuations of a weakly diffusive passive plume in a turbulent boundary  
365 layer, *Boundary-Layer Meteorol.* 64 (1993) 321–354.
- 366 [14] R. M. Gailis, A. Hill, E. Yee, T. Hilderman, Extension of a fluctuating  
367 plume model of tracer dispersion to a sheared boundary layer and to a  
368 large array of obstacles, *Bound.-Lay. Meteorol.* 122 (2007) 577–607.
- 369 [15] E. Yee, A. Skvortsov, Scalar fluctuations from a point source in a tur-  
370 bulent boundary layer, *Phys. Rev. E* 84 (2011) 036306.
- 371 [16] C. Nironi, P. Salizzoni, M. Marro, P. Mejean, N. Grosjean, L. Soulhac,  
372 Dispersion of a passive scalar fluctuating plume in a turbulent boundary  
373 layer. Part I: Velocity and concentration measurements, *Bound.-lay.*  
374 *Meteorol.* 156 (2015) 415–446.

- [17] G. Efthimiou, S. Andronopoulos, I. Toliás, A. Venetsanos, Prediction of the upper tail of concentration distributions of a continuous point source release in urban environments, *Environ. Fluid Mech.* 16 (2016) 899–921.
- [18] M. Bertagni, M. Marro, P. Salizzoni, C. Camporeale, Solution for the statistical moments of scalar turbulence, *Phys. Rev. Fluids* (2019).
- [19] M. Abramowitz, I. Stegun, Handbook of mathematical functions: with formulas, graphs, and mathematical tables, volume 55, Courier Corporation, 1965.
- [20] E. Villermaux, J. Duplat, Mixing as an aggregation process, *Phys. Rev. Lett.* 91 (2003) 184501.
- [21] J. Duplat, E. Villermaux, Mixing by random stirring in confined mixtures, *J. Fluid Mech.* 617 (2008) 51–86.
- [22] M. Brancher, K. D. Griffiths, D. Franco, H. de Melo Lisboa, A review of odour impact criteria in selected countries around the world, *Chemosphere* 168 (2017) 1531–1570.
- [23] R. Scorer, *Air Pollution*, Pergamon Press, 1972.
- [24] U. Högström, A method for predicting odour frequencies from a point source, *Atmos. Environ.* 6 (1972) 103–121.
- [25] L. Kristensen, J. Weil, J. Wyngaard, Recurrence of high concentration values in a diffusing, fluctuating scalar field, in: *Boundary Layer Studies and Applications*, Springer, 1989, pp. 263–276.
- [26] E. Yee, P. Kosteniuk, G. Chandler, C. Biltoft, J. Bowers, Recurrence statistics of concentration fluctuations in plumes within a near-neutral atmospheric surface layer, *Boundary-Layer Meteorology* 66 (1993) 127–153.
- [27] S. O. Rice, Mathematical analysis of random noise, *Bell System Technical Journal* 23 (1944) 282–332.
- [28] E. Yee, An analytical model for threshold crossing rates of concentration fluctuations in dispersing plumes, *Bound.-lay. Meteorol.* 98 (2000) 517–527.

- 406 [29] E. Yee, P. Kosteniuk, G. Chandler, C. Biltoft, J. Bowers, Statistical  
407 characteristics of concentration fluctuations in dispersing plumes in the  
408 atmospheric surface layer, *Bound.-lay. Meteorol.* 65 (1993) 69–109.
- 409 [30] S. Du, D. J. Wilson, E. Yee, A stochastic time series model for thresh-  
410 old crossing statistics of concentration fluctuations in non-intermittent  
411 plumes, *Bound.-lay. Meteorol.* 92 (1999) 229–241.
- 412 [31] T. Hilderman, D. Wilson, Simulating concentration fluctuation time  
413 series with intermittent zero periods and level dependent derivatives,  
414 *Bound.-lay. Meteorol.* 91 (1999) 451–482.
- 415 [32] A. R. Jones, D. J. Thomson, Simulation of time series of concentra-  
416 tion fluctuations in atmospheric dispersion using a correlation-distortion  
417 technique, *Bound.-lay. Meteorol.* 118 (2006) 25–54.
- 418 [33] M. Cassiani, P. Franzese, J. Albertson, A coupled Eulerian and La-  
419 grangian mixing model for intermittent concentration time series, *Phys.*  
420 *Fluids* 21 (2009) 085105.
- 421 [34] L. Ridolfi, P. D’Odorico, F. Laio, Noise-induced phenomena in the en-  
422 vironmental sciences, Cambridge University Press, 2011.
- 423 [35] F. Gifford, Statistical properties of a fluctuating plume dispersion model,  
424 in: *Adv Geophys*, volume 6, Elsevier, 1959, pp. 117–137.
- 425 [36] F. Laio, A. Porporato, L. Ridolfi, I. Rodriguez-Iturbe, Mean first passage  
426 times of processes driven by white shot noise, *Phys. Rev. E* 63 (2001)  
427 036105.
- 428 [37] B. Sawford, Micro-mixing modelling of scalar fluctuations for plumes in  
429 homogeneous turbulence, *Flow, Turbul. Combust.* 72 (2004) 133–160.
- 430 [38] M. Cassiani, P. Franzese, U. Giostra, A PDF micromixing model of  
431 dispersion for atmospheric flow. Part I: development of the model, ap-  
432 plication to homogeneous turbulence and to neutral boundary layer,  
433 *Atmos. Environ.* 39 (2005) 1457–1469.
- 434 [39] S. Arya, *Air pollution meteorology and dispersion*, volume 6, Oxford  
435 University Press New York, 1999.

- 436 [40] G. I. Taylor, Diffusion by continuous movements, P. Lond. Math. Soc.  
437 2 (1922) 196–212.
- 438 [41] H. Tennekes, J. L. Lumley, First Course in Turbulence, Cambridge,  
439 Mass. MIT Press, 1972.
- 440 [42] S. Pope, Turbulent flows, Cambridge university press, 2000.
- 441 [43] M. Cassiani, A. Radicchi, J. Albertson, U. Giostra, An efficient algo-  
442 rithm for scalar PDF modelling in incompressible turbulent flow; numer-  
443 ical analysis with evaluation of IEM and IECM micro-mixing models,  
444 J. Comput. Phys. 223 (2007) 519–550.
- 445 [44] M. Marro, P. Salizzoni, L. Soulhac, M. Cassiani, Dispersion of a pas-  
446 sive scalar fluctuating plume in a turbulent boundary layer. Part III:  
447 Stochastic modelling, Bound.-lay. Meteorol. 167 (2018) 349–369.
- 448 [45] P. Franzese, Lagrangian stochastic modeling of a fluctuating plume in  
449 the convective boundary layer, Atmos. Environ. 37 (2003) 1691–1701.
- 450 [46] G. L. Iacono, A. M. Reynolds, Modelling of concentrations along a  
451 moving observer in an inhomogeneous plume. biological application:  
452 model of odour-mediated insect flights, Environmental Fluid Mechanics  
453 8 (2008) 147–168.
- 454 [47] D. J. Wilson, Concentration fluctuations and averaging time in vapor  
455 clouds, John Wiley & Sons, 2010.
- 456 [48] P. Chatwin, P. J. Sullivan, The intermittency factor of scalars in turbu-  
457 lence, Phys. Fluids A-Fluid 1 (1989) 761–763.
- 458 [49] C. McHugh, D. Carruthers, H. Edmunds, Adms–urban: an air quality  
459 management system for traffic, domestic and industrial pollution, Int.  
460 J. Environ. Pollut. 8 (1997) 666–674.
- 461 [50] A. J. Cimorelli, S. G. Perry, A. Venkatram, J. C. Weil, R. J. Paine, R. B.  
462 Wilson, R. F. Lee, W. D. Peters, R. W. Brode, Aermol: A dispersion  
463 model for industrial source applications. part i: General model formula-  
464 tion and boundary layer characterization, J. App. Meteorol. 44 (2005)  
465 682–693.

- 466 [51] E. Yee, R. Chan, P. Kosteniuk, G. Chandler, C. Biltoft, J. Bowers,  
467       Measurements of level-crossing statistics of concentration fluctuations  
468       in plumes dispersing in the atmospheric surface layer, *Bound.-layer*  
469       *Meteor.* 73 (1995) 53–90.